

1 **DEVELOPMENT AND EXPERIMENTAL VALIDATION OF A MONTE CARLO**
2 **MODELING OF THE NEUTRON EMISSION FROM A d-t GENERATOR**

3
4 **Authors:** Romolo Remetti¹ , Luigi Lepore¹ , Nadia Cherubini²,

5 **Affiliations:**

6 1) Sapienza University of Rome, Dept. SBAI, Via Antonio Scarpa 14, 00161 Rome, Italy

7 2) ENEA CRE Casaccia, Nuclear Material Characterization Laboratory and Nuclear Waste
8 Management, Via Anguillarese 301, 00123 Rome, Italy

9
10 **KEYWORDS:** Neutron Generator, Neutron Emission, MCNPX, Thermo Scientific MP320

11
12
13 **ABSTRACT**

14 An extensive use of Monte Carlo simulations led to the identification of a Thermo Scientific
15 MP320 neutron generator MCNPX input deck. Such input deck is currently utilized at ENEA
16 Casaccia Research Center for optimizing all the techniques and applications involving the
17 device, in particular for explosives and drugs detection by fast neutrons.

18 The working model of the generator was obtained thanks to a detailed representation of the
19 MP320 internal components, and to the potentialities offered by the MCNPX code.

20 Validation of the model was obtained by comparing simulated results vs. manufacturer's data,
21 and vs. experimental tests.

22 The aim of this work is explaining all the steps that led to those results, suggesting a procedure
23 that might be extended to different models of neutron generators.

24
25
26 **1. INTRODUCTION**

27 Neutron generators are one of the most widespread sources of fast neutrons for different kind of
28 elemental analyses applications, ranging from the quantitative estimation of the fissile/fertile
29 materials in radioactive wastes packages, to the interrogation of containers suspected of
30 containing illicit substances, like explosives or drugs.

31 To put in place a particular application some quantities have to be optimized, such as the neutron
32 energy needed, and the neutron output rate required. High energy neutrons (> 10 MeV) and high
33 neutron emission rates ($>10^8$ n/s) means the use of the ${}^2\text{H}(t,n){}^4\text{He}$ fusion reaction, that produces,
34 theoretically, 14.1 MeV neutrons. If lower energies are required (< 3 MeV), the ${}^2\text{H}(d,n){}^3\text{He}$
35 fusion reaction is available, but with lower efficiency in production rate: commercial neutron
36 generators based on d-d reaction do not exceed $5\cdot 10^7$ n/s, usually. Anyway, lower energies
37 neutrons can be produced by d-t systems also, by slowing-down the 14.1 MeV neutrons. The best
38 solution has to be evaluated case by case.

39 Focusing on neutron angular emission, the d-t fusion process produces neutrons with a few
40 percent anisotropy: because of the slightness of this effect the emission could be considered
41 without any preferential direction, but as a first approximation only. In other words, the neutron
42 generator internal target, in which fusion reactions occur, could certainly be considered as an
43 isotropic source, but, as soon as neutrons leave the target, their first interactions happen with the
44 generator's internal materials, causing scattering from their original trajectories. Summarizing,
45 the neutron distribution vs. solid angle modifies itself in a way that is peculiar to the internal
46 layout of the specific generator.

47 When performing R&D activities for measurement techniques based on neutron interrogation, in
48 order to get an accurate evaluation of the source term, and its effect on the measurement of
49 concern, it is mandatory to perform preliminary calibrations aimed at determining neutron's
50 average energy, and flux, at determined angular positions vs. the generator's working
51 parameters, such as supply voltage, ion beam current, frequency of the pulses, and duty factor.
52 Typically, this is obtained by means of costly and time-consuming experimental calibrations.
53 Monte Carlo simulation codes, when reproducing satisfactorily the angle-energy distribution of
54 neutrons, may represent a powerful mean for reducing the experimental efforts of the calibration
55 phase.

56 Other works concerning neutron generator simulations have been published so far, for instance
57 concerning distribution of fusion products [1], neutron fluxes calculation outside
58 shielding/moderating structures encompassing the generator [2], and dosimetric field around the
59 generator itself [3]. The main target of this work is obtaining a designing tool allowing to
60 estimate what is the neutron flux impinging on a measurement system placed at a fixed point

61 respect to the generator, and to calculate how neutron flux changes vs. generator's working
62 parameters.

63

64 The neutron generator considered for this work is the d-t Thermo Scientific MP-320. This system
65 is rugged, very compact, portable and light in weight. It is based on a deuterium-tritium sealed
66 source and it is designed for laboratory or field applications. It generates a maximum of 10^8 n/s
67 and it is capable of continuous or pulsed output, the latter ranging from 500 Hz to 20 kHz.

68 According to the needs of the user, the MP-320 can be provided either for d-t and d-d fusion
69 sources. More details about the device and its capabilities can be found in [4].

70 In the current research, the techniques the neutron generator is involved in require the employ of
71 fast neutrons, e.g. Differential Die Away-time Analysis (DDAA), [5], for fissile and fertile
72 recognition and quantification, and Fast Neutron Analysis (FNA), [6], for explosive detection. It
73 means that the generator is used mainly unshielded, inside an appropriate bunker for radiation
74 protection issues. In these conditions, devising the neutrons behavior with materials of concern
75 is strictly function of the source term characterization, and a classical interpretation of the
76 neutron generator as a point source, that is usually acceptable when the neutron generator is
77 embedded into a thermalizing moderating structure, could be unsatisfactory. Since reference data
78 from the manufacturer, and first experimental characterizations carried out at ENEA Casaccia
79 Research Centre, had shown significant neutron flux depressions at certain angular positions, it
80 was decided to develop a Monte Carlo model capable both to explain such an anisotropy, and to
81 foresee its modifications when varying generator's working parameters.

82

83 **2. METHODOLOGY**

84 Currently, the most efficient method to simulate the neutron production by a neutron generator is
85 the Monte Carlo simulation. By this approach, a lot of 'histories' of the particle of interest are
86 run, in order to reproduce, into a virtual world, all the possible paths traveled by the radiation, by
87 means of random samplings from all the probability density functions ruling physical
88 phenomena. Very complex geometries can be built, and very accurate results can be produced if
89 the user puts into the calculation all the elements important to the transport of the analyzed
90 radiation; moreover, a sufficient computational power should be available for running a
91 statistical significant number of histories.

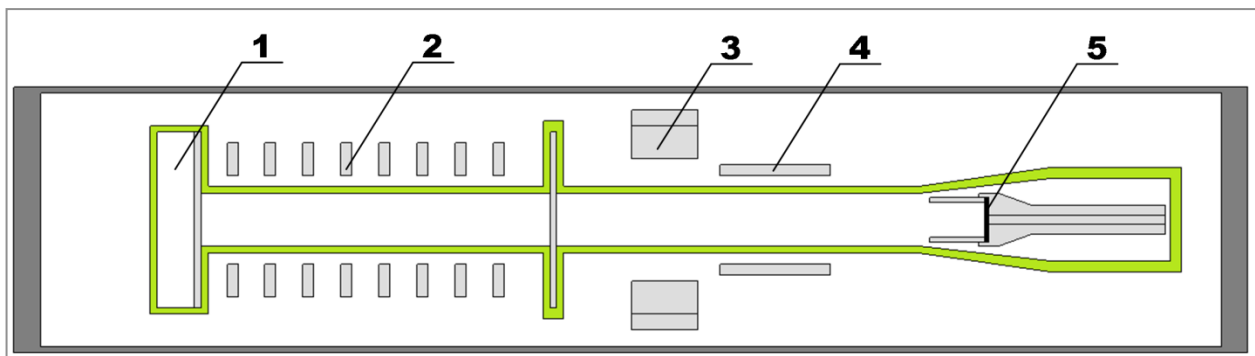
92 For this work, the MCNPX (Monte Carlo N-Particle eXtended) code has been used, in its version
93 MCNPX 2.7.0. [7]. By default, the code is able to transport deuterium and tritium ions inside the
94 matter, but it does not treat the fusion reaction between those isotopes. For overcoming such a
95 difficulty, a subroutine based on a fusion source model developed by Pillon et al. [8] has been
96 added to the code, by proper re-compilation of MCNPX source code.

97 As stated by Pillon et al., the d-t fusion neutrons, produced by the ion beam-target interaction,
98 show angle-energy dependence, as well as spatial anisotropy. For each neutron which is sampled,
99 MCNPX obtains from the source-model subroutine the following information: *i)* the direction
100 cosines (u, v, w) , which establish the neutron emission direction, *ii)* the neutron energy (E), and
101 *iii)* the particle weight W_n , [8]. The neutrons produced show few hundred keV spread around the
102 theoretical 14.1 MeV, and few percent anisotropy vs. the angle of emission. It's worth to note
103 that, for its correct application, the fusion source subroutine needs input data, such as the
104 generator's target material, its dimensions and layers, the focal spot dimension, and the ion beam
105 acceleration voltage. In particular, it is important to remark that the MCNPX source term was not
106 modeled with the usual SDEF card. The fusion source subroutine considers a cylindrical tritium
107 target with four-six coaxial layers. According to geometry and density of each layer, to the
108 acceleration voltage, and to the focal spot, the subroutine calculates the points where fusion occurs
109 on the basis of deuteron's range within the target itself. Once the starting point is fixed, neutron
110 direction cosines, energy, and weight, are determined. Being the generator new, a fully loaded
111 target was considered. To account for progressive depletion, periodical recalibrations have to be
112 foreseen.

113 By the way, it is interesting to note that, by the same methodology, a source model for d-d fusion
114 reaction has been developed also, [9], with the final aim to treat all the aspects relating to fusion
115 processes and fusion generators.

116 By integrating the fusion source model into MCNPX, and having considered the successive
117 interactions of fusion neutrons inside the generator, it was possible to achieving a reliable Monte
118 Carlo model of the Thermo Scientific MP-320 neutron generator [4], capable to reproduce the
119 real neutron emission from the device. Apart from the use of the source model subroutine, the
120 key issue for achieving such a result was the simulation of the generator's internal components
121 relevant for neutron transport. The need for simulating generator's internal components was
122 suggested by the documentation provided by the manufacturer of MP-320 [10]. A first

123 comparison with an equivalent 14.1 MeV point isotropic source , intended as the simplest model
 124 for a d-t neutron generator, suggested that a more reliable MCNPX model could be developed to
 125 reproduce the angular emission given by the manufacturer. It should be noted that, as declared by
 126 the manufacturer, data on angular emissions had been originated by his own MCNP calculations.
 127 If schematics of the generator's internal structure had been previously known, no particular effort
 128 would have been required, but no schematics of the internal structure were available. Because of
 129 that, information have been crossed from the device's operation manual [11] and a IAEA
 130 document on the subject, [12]. The guessed internal structure of the generator has been adjusted,
 131 during the sequence of the simulations, in order to reproduce the neutron flux vs. the azimuth
 132 angle as rated by the manufacturer. With the information crossed by the references cited
 133 previously, about 45 sequential trials have been run to achieve a model capable of reproducing
 134 the real emission by the device accurately. The final working structure is presented in Figure 1.
 135



136 Figure 1 ThermoScientific MP-320 neutron generator guessed internal structure: 1) ion source and extractor lens; 2) pulser; 3) focus lens; 4) accelerator; 5) tritiated target.

137
 138 From the figure, following the path of deuterium ions, it is possible to indentify:
 139 1) an ion chamber for producing deuterium/tritium ions, coupled with an extractor lens for
 140 leading ions into the acceleration section;
 141 2) the pulser;
 142 3) a focus lens for shaping the deuterium beam;
 143 4) the acceleration section;
 144 5) the tritium-doped target.

145 The order listed before is particular of Thermo-Scientific MP320 neutron generator, and it has
146 not to be intended as mandatory. Other instruments could use more components, or their order
147 could be modified according to the aims to be achieved.

148 Once a good agreement between neutron angular flux by the MCNPX authors' model, and
149 neutron angular flux by the MCNPX manufacturer's model, was achieved (Figure 2), the input
150 deck retrieved has been used in field for experimental validations, as described below.

151 About computational power, the 45 sequential trials did not require particular efforts. For
152 instance, 0.5 h-core per run was sufficient to get significant results with errors <10%, because
153 generator's geometry is quite small.

154 Instead, high computational power may be needed when the user has to simulate the technique
155 involving the use of neutrons. For instance, shielding, large geometries, high resolution in the
156 energy and time domains, usually require the availability of HPC (High Parallel Computing)
157 resources to achieve significant results in reasonably short time. For instance, the validation
158 phase for the neutron generator model into the "Neutron Bunker" of Figure 5 needed about 500
159 h-core per simulation, due to the large masses of material the neutrons are interacting with.

160 The computing resources and the related technical support used for this work, and all future uses,
161 are provided by CRESCO/ENEAGRID High Performance Computing infrastructure [13].

162 CRESCO/ENEAGRID High Performance Computing infrastructure is funded by ENEA, and by
163 Italian and European research programmes [14].

164

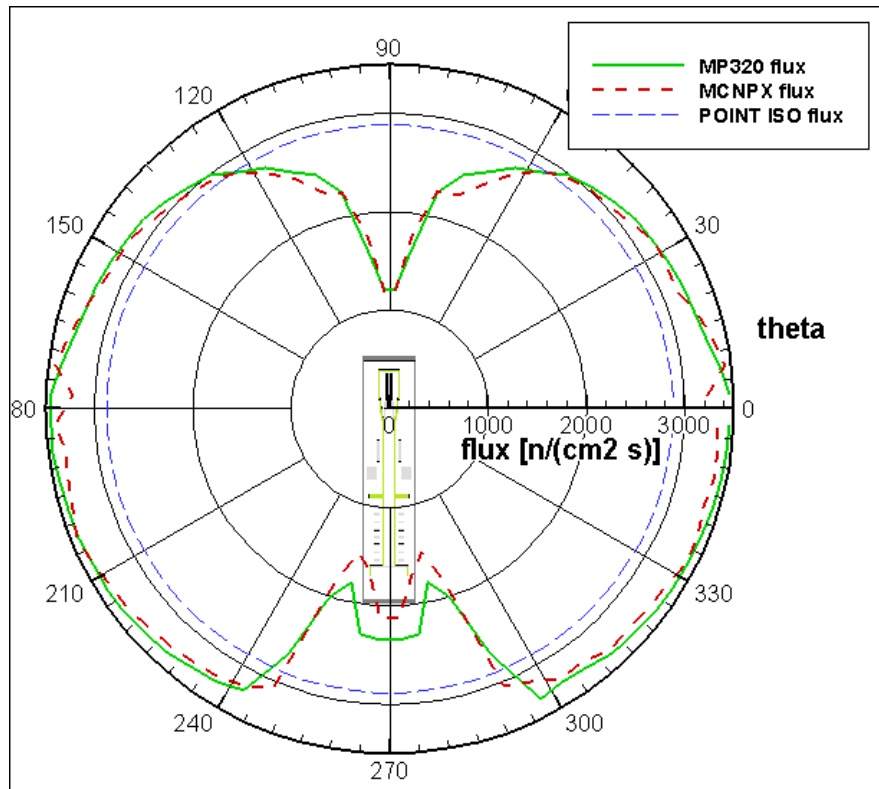
165 2.1 Development of the neutron generator model

166 As materials are concerned, copper, iron, aluminum and aluminum oxide (alumina), especially in
167 massive components, were assumed to be important for neutrons' scattering inside the device,
168 while thin parts were neglected.

169 A first indication was given by the neutron flux angular distribution rated by manufacturer [10]
170 via his proprietary MCNP input deck of the device: such data are reported in Figure 2. It should
171 be noted that the angular flux has been calculated in a free-in-air condition: it means that the
172 curve is not affected by secondary effects of interactions of the neutrons emerging from the
173 generator with any structure. Such a condition is referred by the authors as 'uncollided flux'.

174 A set of 45 sequential trials was needed to develop the neutron generator model, as to reproduce,
175 via MCNPX simulation, the neutron angular distribution given by the manufacturer in the

176 corresponding free-in-air conditions. The comparison of the model results vs. manufacturer's one
177 is given in Figure 2.



178

Figure 2 Comparison between the uncollided angular neutron emission, over all energies, by the MP320 neutron generator's MCNP model from the manufacturer (@ 50 cm far from the center of the target) and the angular flux calculated by the MCNPX model by the authors. For comparison, the uncollided angular neutron flux corresponding to the hypothesis of a 14.1 MeV isotropic point source is added.

179

180 With reference to Figure 2, maximum deviations from isotropy of the neutron flux vs. azimuthal
181 angle happen at $\theta=90^\circ$ and $\theta=270^\circ$, in correspondence to the end-caps of the generator tube.

182 From the shape of these neutron flux deviations, useful information about the internal layout
183 were derived.

184 Referring to Figure 2, focusing on the $\theta=90^\circ$ flux depression, it is clear that this modification is
185 caused by:

- 186 • the alumina electric insulator of the electrode which drives the supply voltage to the
187 doped target (the conical component sustaining item #5 in Figure 1);
- 188 • the copper electrode sustained by the alumina insulator.

189

190 It is evident from Figure 2 that the agreement between MCNPX calculations by the authors and
191 the MCNP data given by the supplier is satisfactory.

192 It should be noted that an eventual hypothesis of considering the neutron generator as a point
193 source of 14.1 MeV neutrons, without considering the interaction of fusion neutrons with
194 generator's internals, leads to deceptive results for neutron flux. As observed in Figure 2, the
195 generator's internals cause a deflection of neutrons emerging from the target, depleting the
196 emission in some angles, and enriching in some others. For instance, when considering the same
197 neutron yield, at $\theta=0^\circ$ the neutron flux given by the accurate MCNPX model of the generator
198 results 15% higher than that from isotropic point source assumption.

199 Use of moderating materials could certainly hide such a difference, but for DDAA and FNA
200 techniques the neutron generator's use is mainly unshielded.

201 From Figure 2, it may be observed that around $\theta=270^\circ$, the neutron flux behavior is more
202 complex: two local minima can be noticed.

203 Such a behavior is due to:

- 204 • the copper coils of the pulser (item #2 of Figure 1) ;
- 205 • the conductive/ferromagnetic parts of the focus lens and the accelerator (item #3, #4 of
206 Figure 1).

207 The maximum at $\theta=270^\circ$ is due to neutrons that travel from the target (item #5 of Figure 1) to
208 the deuterium source (item #1 of Figure 1) in the void central channel of the generator.

209 It is evident from Figure 2 that, in this case, the agreement between MCNPX calculation by the
210 authors and the MCNP data given by the supplier is less accurate: although the trend is the same,
211 an appreciable bias is present. Anyway, further improvements of the model were not carried out,
212 because the $\theta=270^\circ$ position is not involved with the current foreseen utilization of the generator.

213 About neutron yield, given that the manufacturer certifies the neutron output for a single setting
214 of the generator (80 kV voltage of the accelerator, and 60 μA deuteron current, that corresponds
215 to the maximum yield of $1.1 \cdot 10^8$ n/s $\pm 25\%$ [15]), the Monte Carlo model allows to calculate the
216 neutron production for every other settings by scaling down.

217 Current and voltage of neutron generators are the main working parameters to the neutron output
218 rate. For the MP-320, they can be set into the range of 20-60 μA for the ion current, and 40-80
219 kV for the acceleration voltage. The neutron rate vs. ion current is generally quite linear. Instead,
220 for the neutron rate vs. acceleration voltage, the manufacturer suggests a dependency

221 proportional to $\sim V^{1.5}$. Actually, this relationship is more complex, and can be derived by using
222 the MCNPX modelization of the generator by combining the following data:

223 • the target construction data. For instance:

224 – thickness and density;

225 – doped depth;

226 – doping concentration;

227 – diffusion processes;

228 – ageing.

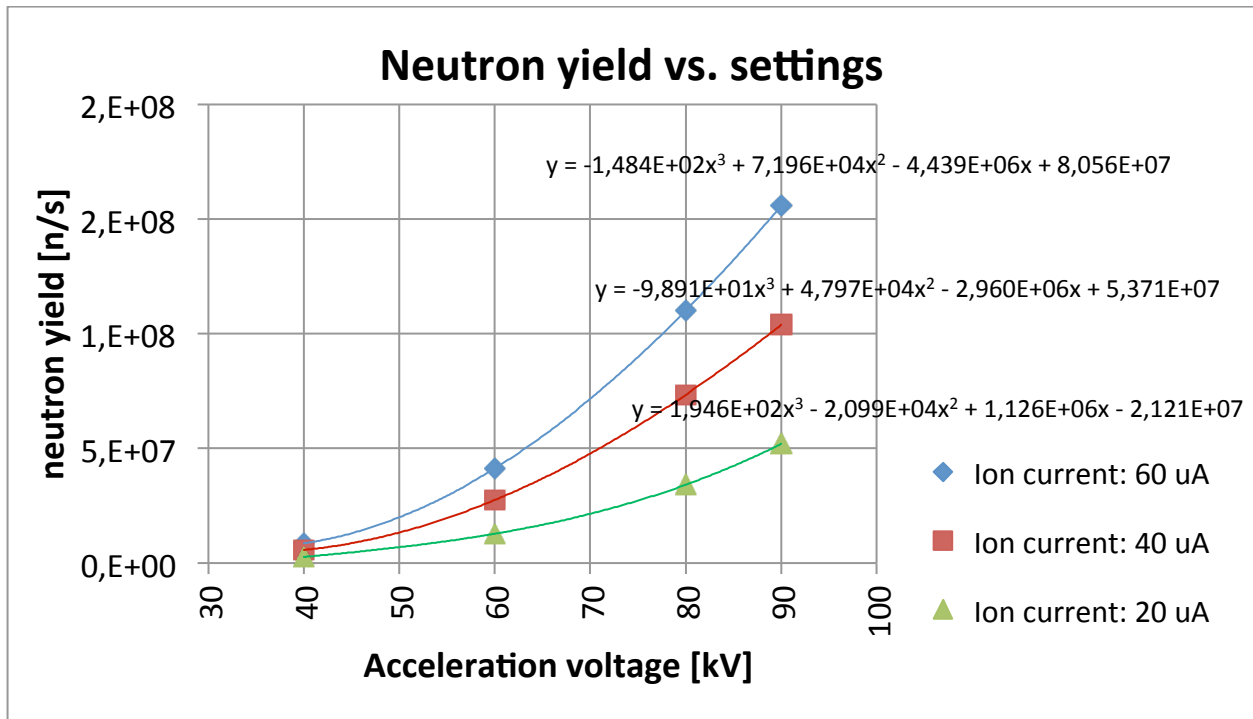
229 • the penetration capabilities and interaction rate of the ion accelerated on the target.

230 Because of that, amid the set of MP320 generators built by the manufacturer, the neutron rate
231 emission vs. the acceleration voltage is specific for each single item.

232 By means of the Monte Carlo approach used before, and thanks to the source subroutine by
233 Pillon et al. [8], by knowing only the single emission rate from the calibration certificate by the
234 supplier, it was assumed the possibility to calculate the emission rate corresponding to other
235 working points, by normalizing the model results to the known point.

236 Because MCNPX results are normalized per source particle, for reproducing the device's output,
237 it is necessary to adopt a normalization factor derived from manufacturer's data. The results of
238 such a calculation are shown below.

239



240

Figure 3 Thermo Scientific MP-320 neutron yields vs. accelerator voltage and deuteron beam current. Obtained via simulations calibrated with the manufacturer certificate [15]. 25% uncertainty on neutron yield should be considered, according to the uncertainty given by the manufacturer for the calibration point (60 μ A @ 80 kV).

241

242 Figure 3 shows the variation of neutron yield vs. accelerator voltage for three current values. It is
 243 worth to remark that the supplier gives the output rate corresponding to the maximum yield only
 244 (60 μ A @ 80 kV), with a 25% uncertainty. It should be noted that such uncertainty is propagated
 245 to the MCNPX predicted neutron yield via the normalization told before. Monte Carlo
 246 calculation errors are practically reduced to zero by running a very high number of histories (*nps*
 247 more than 10^9).

248 Such a procedure is to be intended as an integration of the manufacturer's information, and
 249 allows the user to determine the optimal setting parameters for obtaining the desired neutron
 250 yield. Figure 3 shows three curves but only one is really relevant, because the other ones result
 251 proportional by means of the ion beam current. Reporting all three lines into the graph is
 252 intended as a practical aid for the operator, for helping to select the appropriate neutron
 253 generator's working parameters according to the desired neutron output.

254

255

256 **3. EXPERIMENTAL VALIDATION**

257 An experimental setup has been realized at ENEA Casaccia “Nuclear Material Characterization
258 Laboratory and Nuclear Waste Management” [16] in order to validate the simulated results. In
259 particular for:

260 1) the emission at $\theta=0^\circ$, (Figure 2), with generator operated at its maximum neutron yield (60
261 $\mu\text{A @ 80 kV}$);

262 2) the emission at $\theta=0^\circ$, (Figure 2), with generator operated at its minimum neutron yield (20
263 $\mu\text{A @ 40 kV}$).

264

265 The $\theta=0^\circ$ position, corresponding to the spot of maximum neutron flux, was used for the
266 particular laboratory’s arrangement for implementing DDAA and FNA.

267 The code validation has been carried out as follows:

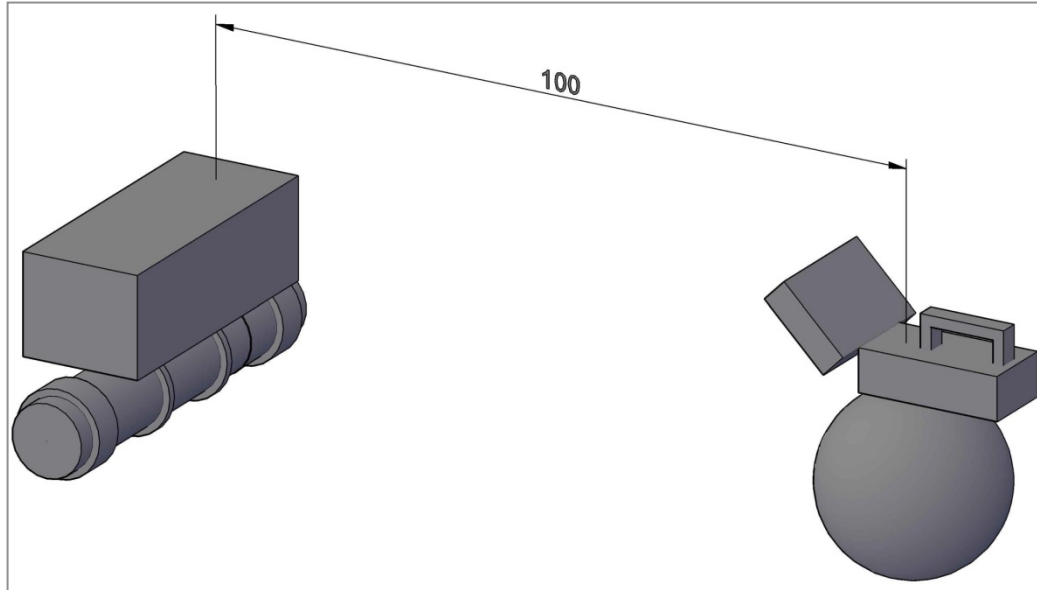
268 1) accurate reproduction of the measurement condition’s geometry and materials into
269 MCNPX;

270 2) comparison of predicted neutron yields by the MCNPX neutron generator model vs.
271 neutron yields measured in field at the minimum and maximum power, respectively (20
272 $\mu\text{A @ 40 kV}$) and (60 $\mu\text{A @ 80 kV}$).

273

274 The experimental neutron rate vs. generator’s main operating parameters has been measured by
275 means of a Berthold LB6411 neutron counter, in the geometrical configuration shown in Figure
276 4.

277



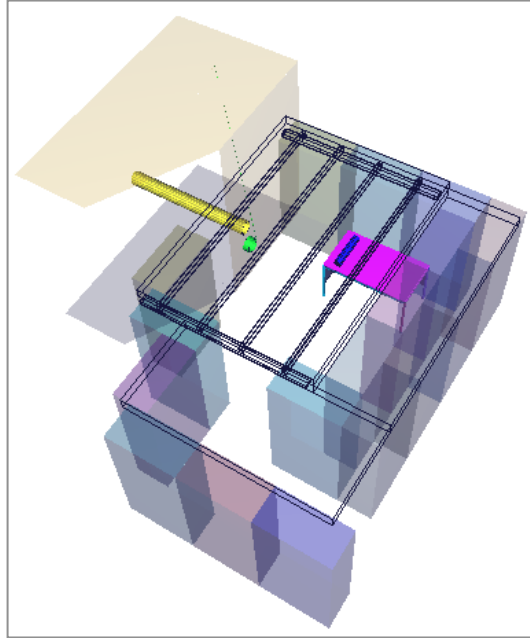
278

Figure 4 Experimental setup for Thermo Scientific MP-320 neutron generator and Berthold LB6411 neutron counter. Dimensions are expressed in cm.

279

280 As needed for obtaining accurate results from Monte Carlo calculations, MCNPX input included
281 geometries and materials of the room where experimental measurements took place, as well as
282 structural materials, *e.g.* walls, floor, table holding the generator, which could significantly affect
283 the flux distribution. In particular, Figure 5 gives a description of the “neutron bunker” of the
284 ENEA Casaccia TRIGA RC-1 reactor building, where measurements have been carried out.
285 Walls and floor are made of ordinary or baritic concrete, while the ceiling is made of
286 polyethylene sheets supported by steel beams. Other elements, *e.g.* the LB6411, other
287 components of the neutron plug, P.E. and lead bricks present inside the bunker, were included
288 into the simulation, but neglected in the representation given in Figure 5 for clarity of
289 representation.

290



291

Figure 5 The “Neutron Bunker” where measurements have been carried out, as simulated in MCNPX Visual Editor. The generator (the blue cylinder) is laid on the table together with neutron counter (not represented). Together with the walls (gray boxes), and the ceiling (wireframe boxes), the reactor diametral thermal channel’s water neutron plug (yellow and green cylinders) is represented.

292

293 Summarizing, the geometry of the experimental measurement has been reproduced into MCNPX
 294 very accurately, in order to get the same total detection efficiency as the real experimental test.

295 About simulation details, 10^{10} neutron histories were considered, with computational efforts in
 296 the order of 500 h-core per simulation due to complexity and overall dimensions of the geometry.

297 Regarding the experimental phase and focusing on the measurement of the maximum neutron
 298 yield by MP-320, having set the generator at (60 μ A @ 80 kV) in a continuous irradiation mode,
 299 five count rates from Berthold LB6411 were registered. The averaged result was 1645 cps \pm 2%.

300 As known, LB6411 can be used to estimate the neutron flux, at the position where it is placed, by
 301 means of a conversion factor, called ‘ R ’ by detector’s operating manual. R is function of the
 302 neutron spectrum entering the polyethylene sphere. According to the operating manual, the
 303 knowledge of the neutron spectrum is used to get a more accurate evaluation of R . It is obtained
 304 by weighting the function $R(E)$ on neutron energy spectrum, $\varphi(E)$, entering the detector,

305

$$R = \frac{\int R(E) \cdot \varphi(E) dE}{\int \varphi(E) dE}$$

306

307 It is worth to note that the R default value, stored in the detector, refers to ^{252}Cf spontaneous
308 fission neutrons energy spectrum. R unit is cm^2 ; when count rate is divided by R , the local
309 neutron flux is calculated.

310 As can be easily seen, while the count rate is retrieved experimentally, R cannot be evaluated
311 directly by LB6411. The availability of the ‘Neutron Bunker’ (Figure 5) MCNPX input deck,
312 shown before, can overcome the gap providing a computation of the required energy spectrum.

313 In order to evaluate the goodness of the MP-320 neutron generator model developed, two
314 calculations have been carried out starting from the experimental count rates $1645 \text{ cps} \pm 2\%$
315 given by LB6411:

- 316 1) calculation of factor R , and corresponding generator neutron yield, considering the
317 generator as a 14.1 MeV point isotropic source;
- 318 2) calculation of factor R , and corresponding generator neutron yield, considering the
319 generator model developed.

320

321 The relationship between the measurement by LB6411 and neutron yield is the following

322

$$\text{measured neutron yield} = \frac{\text{measured count rate}}{R \cdot F2 \text{ tally on LB6411}}$$

323

324 where R is the LB6411 correction factor discussed before, and the ‘F2 tally’ is a result of the
325 MCNPX simulation; it physically represents the number of neutron entering the polyethylene
326 sphere of the detector, divided by the number of started neutrons, divided by the detector’s
327 polyethylene sphere surface area.

328 All results are resumed in the following Table 1.

329

	$R [\text{cm}^2]$	F2 tally on LB6411 surface $[\text{cm}^{-2}]$	Measured neutron yield $[\text{n/s}]$	$\Delta\%$ with manufacturer reference
14.1 MeV point isotropic source	5.627E-01	2.238E-05	1.307E+08	+18.8%
MP-320 model by the authors	5.606E-01	2.432E-05	1.207E+08	+9.7%

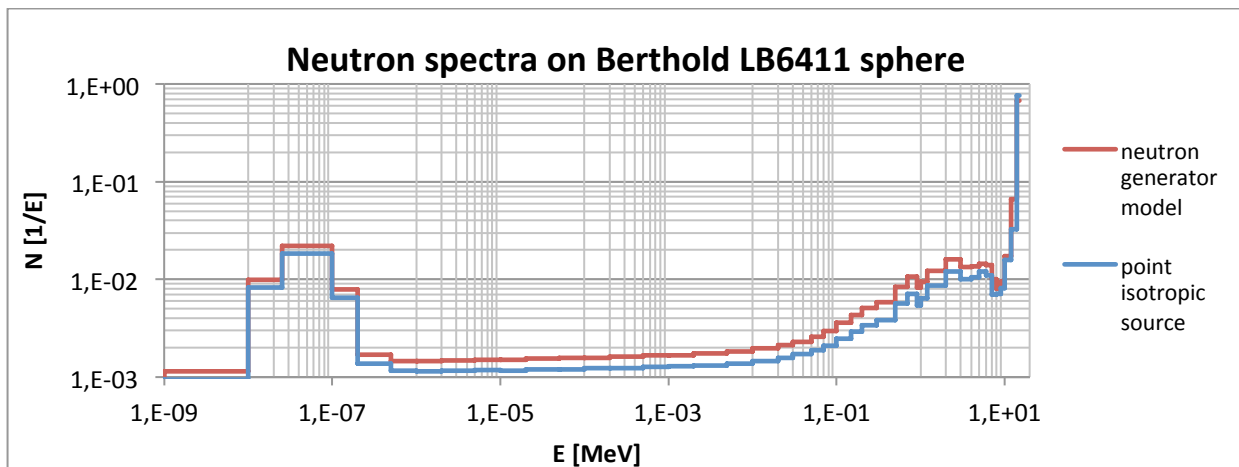
Table 1 Comparison of the measured neutron yield by means of Berthold LB6411 neutron detector vs. the reference $1.1 \cdot 10^8$ n/s rated by manufacturer (60 μ A @ 80 kV).

330

331 Differences in R values and F2 tally values in Table 1 can be explained as follows.

332 Referring to Figure 2, the neutron flux angular distribution given by the accurate MCNPX model
 333 of the generator differs in its shape from isotropic point source assumption: it means that also the
 334 interactions inside the ‘Neutron Bunker’ in Figure 5 will differ. Such differences, that affect both
 335 R and F2 tally values, can be viewed throughout the neutron spectra on LB6411 sphere surface,
 336 as reported in Figure 6 and Table 2.

337



338

Figure 6 Neutron spectra entering the Berthold LB6411 polyethylene sphere inside the ENEA Casaccia TRIGA RC-1 ‘Neutron Bunker’. MCNPX calculations have been run in two cases: neutron generator as a point isotropic source (blue curve), neutron generator as the model proposed by the authors (red curve).

339

Neutron energy range	Neutron generator model	14.1 MeV point isotropic source
0-0.025 eV	6.85%	6.61%
0.025–1 eV	22.10%	21.31%
1–200 eV	4.64%	4.18%
200 eV–1 MeV	15.04%	12.31%
1–12 MeV	18.73%	16.81%
12–15 MeV	32.63%	38.77%

Table 2 Numerical values of the neutron spectrum energy composition entering Berthold LB6411 sphere.

340

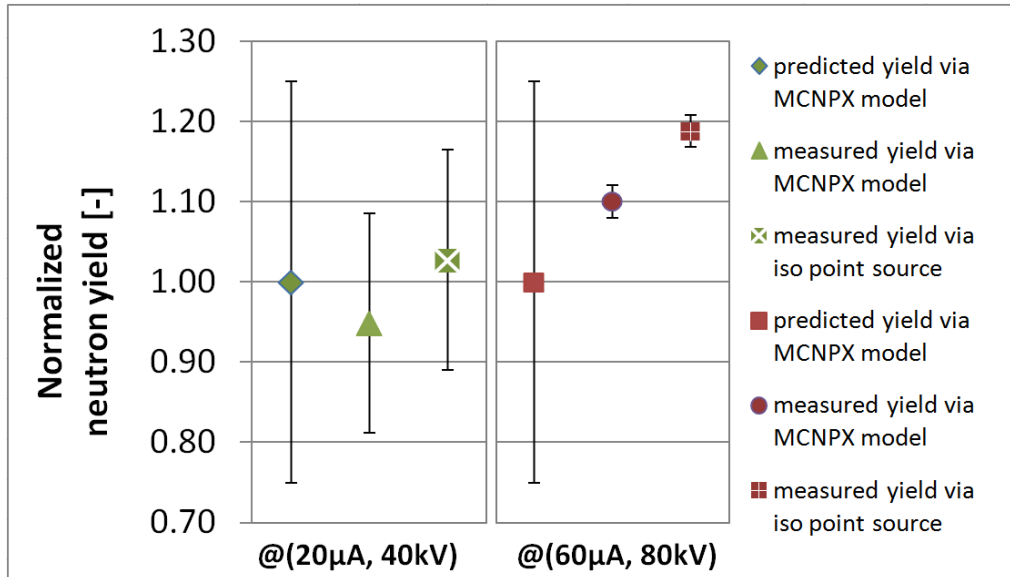
341 The most significant differences in neutron energy spectra can be easily seen in Table 2. Starting
 342 from the first row, the first three energy ranges present almost the same values: multiple
 343 scattering phenomena that produce such a kind of neutrons are due to the “bunker effect”, and
 344 are less dependent on the way the neutron generator output is modeled. The fourth and the fifth
 345 ranges, calculated via the neutron generator model, show larger results than the isotropic point
 346 assumption: that is the effect of the generator ‘internals’ whose primary interactions with 14.1
 347 MeV fusion neutrons deplete the sixth range enriching the forth and the fifth ones. That explains
 348 also why the sixth range results larger for the isotropic point assumption.
 349 The entire procedure shown above has been repeated also for the minimum neutron generator
 350 power. The experimental count rate of LB6411 is 35 cps \pm 13.7%. Applying the appropriate
 351 conversion, measured neutron yield are reported below.
 352

	R [cm ²]	F2 tally on LB6411 surface [cm ⁻²]	Measured neutron yield [n/s]	$\Delta\%$ with MCNPX predicted value
14.1 MeV point isotropic source	5.627E-01	2.238E-05	2.78E+06	+2.7%
MP-320 model by the authors	5.606E-01	2.432E-05	2.57E+06	-5.5%

Table 3 Comparison of the measured neutron yield by means of Berthold LB6411 neutron detector vs. the value $2.71 \cdot 10^6$ n/s predicted by MCNPX model (20 μ A @ 40 kV) calibrated via manufacturer data.

353
 354
 355

A comprehensive representation of results reported in Table 1 and Table 3 is shown in Figure 7.



356

Figure 7 Comparison between the simulated emission rates and measurements at minimum and maximum neutron generator yields. Measured yields have been normalized to predicted values. Measured points are presented according to the different R -correction models.

357

358 At (20 μ A @ 40 kV), the $\Delta\%$ experimental vs. simulated, using both neutron generator model
 359 and isotropic point source assumption, are -5.5% and +2.7% respectively. At (60 μ A @ 80 kV),
 360 the $\Delta\%$ experimental vs. simulated, using both neutron generator model and isotropic point
 361 source assumption, are +9.7% and +18.8% respectively. However, when minimum yield is
 362 measured, counting statistics on LB6411 is poorer than measurements at maximum yields, as can
 363 be graphically seen with uncertainty bars in Figure 7.

364 It is worth to note that

- 365 i) the comparison of experimental vs. simulation measurements at minimum and maximum
 366 yields at $\theta=0^\circ$,
- 367 ii) the agreement among manufacturer angular flux distribution and the angular flux by the
 368 MCNPX model,
- 369 iii) the more likely neutron energy distribution of the MCNPX model vs. the isotropic point
 370 source assumption,

371 increase the confidence in using the input deck developed.

372 Summarizing, the MCNPX model developed, in order to optimize DDAA and FNA techniques,
 373 seems to behave better than the simple isotropic point source.

374

375

376 4. CONCLUSIONS

377 The application of the methodology previously described to the Thermo-Scientific MP-320
378 neutron generator led to the identification of a working MCNPX input deck of the device,
379 capable to reproduce the neutron emission in good agreement vs. measurements.

380 First, a pure simulation procedure has been carried out as to retrieve the generator internal
381 configuration capable in reproducing, in the free-in-air condition, the neutron flux angular
382 distribution given by the manufacturer [10].

383 Once a sufficient agreement has been reached, the MCNPX model, with the features provided by
384 its *ad hoc* neutron source by Pillon et al. [8], has been used to retrieve the operating curve of the
385 device, namely neutron yield vs. settings, via a calibration of the model by means of the
386 manufacturer neutron yield certificate at maximum power.

387 An experimental verification phase has been carried out, measuring the neutron yield at
388 minimum and maximum power by means of a Berthold LB6411 neutron detector. The position
389 selected for the measurement is $\theta=0^\circ$ (Figure 2), being the spot where neutron flux is maximized.

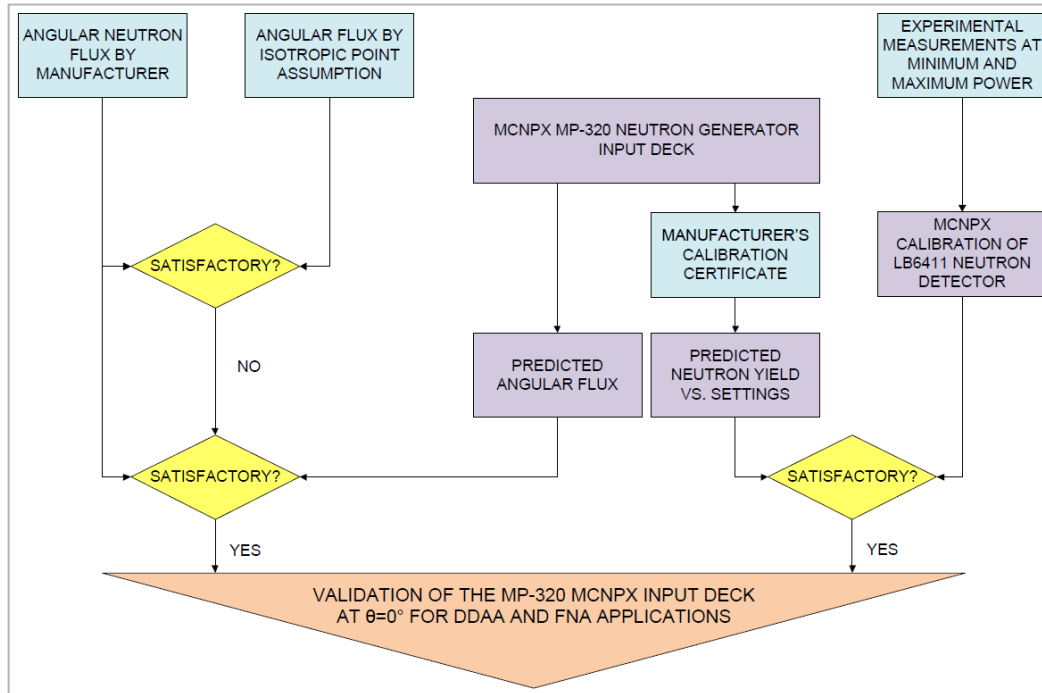
390 The real measurement geometries and materials have been reproduced very accurately into
391 MCNPX as to provide a reliable calibration for LB6411 as to get a valid measurement of the
392 generator neutron yields.

393 Experimental results vs. simulated have been compared: the MCNPX generator model provided
394 by the authors behaves better than 14.1 MeV-isotropic point assumption:

- 395 1) giving more accurate values for the neutron flux at the angular position $\theta=0^\circ$ (Figure 2),
- 396 2) giving more representative neutron spectra at the angular position $\theta=0^\circ$ (Figure 2),
- 397 3) providing a set of operating curves for the device, namely neutron yields vs. settings.

398

399 All described steps are resumed into the workflow presented in Figure 8.



400

Figure 8 Workflow of the study.

401

402 At the current stage of the work, only the $\theta=0^\circ$ geometry has been investigated because DDAA
 403 and FNA setups required the maximum neutron focal spot. Further experimental studies covering
 404 all the theta coordinates are foreseen in the future, in order to carry on another programme
 405 related to activation measurements.

406 The capability of the code allows the user to simulate also the behavior of the device vs. time
 407 when it is used in pulse mode, rather than in continuous neutrons emission. Moreover, it allows
 408 the user to run several trial simulations to optimize measurement technique's geometry and
 409 parameters, powering the generator only to check some correspondence between simulated and
 410 measured values at some key-stages of the technique's optimization process. Feasibility studies
 411 and sensitivity analysis can be implemented in a systematic way, saving precious device's
 412 lifetime.

413 The procedure shown before is very versatile. It can be applied to whatever neutron generator in
 414 order to retrieve a working MCNPX input deck to be implemented for any users' needs.

415 Currently, at ENEA Casaccia Research Center, the realized MCNPX input deck is available for
 416 all the experiments that foresee the use of the MP-320. Further, it will be used in future works on

417 waste assessment and CBRNE (Chemical Biological Radioactive Nuclear and Explosive)
418 activities [17].

419

420

421 **REFERENCES**

422

- [1] U. Wiacek and J. Dankowski, "Monte Carlo modeling of distributions of the d-d and d-t reaction products in a dedicated measuring chamber at the fast neutron generator," *Nuclear Instruments and Methods in Physics Research Section B: Beam Interactions with Materials and Atoms*, vol. 349, pp. 96-102, 2015.
- [2] J. Katalenich, M. Flaska, S. A. Pozzi and M. R. Hartman, "High-fidelity MCNP modeling of a D-T neutron generator for active interrogation of special nuclear material," *Nuclear Instruments and Methods in Physics Research Section A: Accelerators, Spectrometers, Detectors and Associated Equipments*, vol. 652, no. 1, pp. 120-123, 2011.
- [3] J. W. Hayes, E. Finn, L. Greenwood and R. Wittman, "Characterization of a Thermo Scientific D711 D-T neutron generator located in a low-scatter facility," *Nuclear Instruments and Methods in Physics Research Section A: Accelerators, Spectrometers, Detectors and Associated Equipment*, vol. 741, pp. 57-66, 2014.
- [4] Thermo Scientific, "MP 320 Neutron Generators," Thermo Scientific, 2015. [Online]. Available: <http://www.thermoscientific.com/content/tfs/en/product/mp-320-neutron-generators.html>.
- [5] A. C. Raoux, A. Lyoussi, C. Passard, C. Denis, J. Lorida, J. Misraki and P. Chany, "Transuranic waste assay by neutron interrogation and online prompt and delayed neutron measurement," *Nuclear Instruments and Methods in Physics Research Section B*, vol. 207, pp. 186-194, 2003.
- [6] A. Buffler, "Crontraband detection with fast neutrons," *Radiation Physics and Chemistry*, vol. 71, no. 3-4, pp. 853-861, 2004.
- [7] J. F. Briesmeister, "MCNP – A general purpose Monte Carlo code for neutron and photon transport," Nov 1993.
- [8] M. Pillon, M. Angelone, M. Martone and V. Rado, "Characterization of the source neutrons

- produced by the Frascati Neutron Generator,” *Fusion Engineering and Design*, no. 28, pp. 683-688, 1995.
- [9] A. Milocco, A. Trkov and M. Pillon, “A Monte Carlo model for low energy D-D neutron generators,” *Nuclear Instruments and Methods in Physics Research Section B: Beam Interaction with Materials and Atoms*, vol. 271, pp. 6-12, 2012.
- [10] F. Prezzavento, *Private communication*.
- [11] Thermo Scientific, *MP320 Neutron Generator - Operation Manual*.
- [12] IAEA, “Neutron Generators for Analytical Purposes,” Vienna, 2012.
- [13] G. Ponti, “The role of medium size facilities in the HPC ecosystem: the case of the new CRESCO4 cluster integrated in the ENEAGRID infrastructure,” in *2014 International Conference on High Performance Computing and Simulation*.
- [14] ENEA, “ENEA CRESCO Website,” [Online]. Available: <http://www.cresco.enea.it/english> for information..
- [15] Thermo Scientific, *Thermo Scientific MP-320 Neutron Generator calibration certificate*.
- [16] “ENEA, Italian National Agency for New Technologies, Energy and Sustainable Economic Development, website,” [Online]. Available: http://www.enea.it/it?set_language=it&cl=it.
- [17] “End-user driven DEMO for cbrNE,” [Online]. Available: <https://www.eden-security-fp7.eu/>.